Pure & Appl. Chem., Vol. 57, No. 8, pp. 1031–1042, 1985.
Printed in Great Britain.

The structure of aqueous electrolyte solutions as derived from MD (molecular dynamics) simulations

Karl Heinzinger

Max-Planck-Institut für Chemie (Otto-Hahn-Institut),
D-6500 Mainz, Federal Republic of Germany

Abstract - This review concentrates on the structural properties of aqueous electrolyte solutions derived from MD simulations with the ST2 and an improved Central Force model for water. The ion-water pair potentials are either calculated by modelling the ions as Lennard-Jones spheres with an elementary charge at the center or based on ab initio calculations. The concentrations range from 0.55 to 13.9 molal with 200 water molecules in the basic periodic cube. The simulations extended over about 10 ps. The structural properties of the solutions are discussed on the basis of radial distribution functions, the orientation of the water molecules and their geometrical arrangement in the hydration shells of the ions.

INTRODUCTION

In the investigations of complicated liquids - say aqueous electrolyte solutions - which cannot yet be treated analytically, the computer simulations can predict properties which cannot or not directly be measured and they can explain macroscopically measured properties on a molecular level. Another important advantage of an MD simulation is the consistent description in respect to structural and dynamical properties of an aqueous electrolyte solution even if doubts remain on the quantitative significance of single properties because of the uncertainties in the pair potentials employed.

Therefore, decisive for the reliability of the results are the pair potentials employed in the simulation. High accuracy ab initio calculations are not necessarily a guarantee for proper pair potentials as in complicated liquids, such as water, the pair potentials used need to be effective ones, which means that many-body interactions must be incorporated. In this paper the fact is stressed that the best test of the reliability of the pair potentials is the agreement with experimental results as far as they can be deduced unambiguously from measurements.

The results presented here are restricted to structural properties and are derived exclusively from MD simulations because, different from MC calculations, also the dynamical properties of the solutions can be calculated.

In the following section, pair potentials employed in the simulation of aqueous electrolyte solutions are introduced and details of the calculations are given. The structural properties of the solutions are discussed in later sections on the basis of radial distribution functions, the orientation of the water molecules in the hydration shells of the ions and their geometrical arrangement.

EFFECTIVE PAIR POTENTIALS

In the simulations of aqueous electrolyte solutions reported in this paper, the ST2 (ref. 1) and an improved Central Force (CF) (ref. 2) model for water have been employed. The ST2 model is a rigid one, while the CF model consists of oxygen and hydrogen atoms - bearing partial charges - where the water molecule geometry is solely preserved by an appropriate set of oxygen-hydrogen and hydrogen-hydrogen pair potentials. Thus, the CF model has the advantage that the influence of ions on the intramolecular properties of water can be studied.

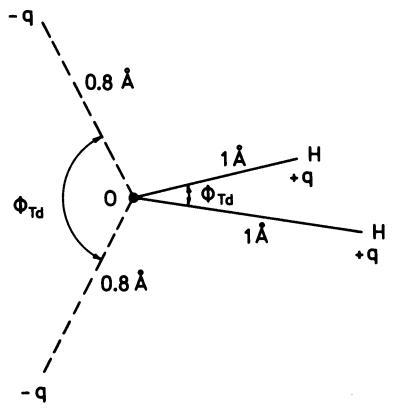

Fig. 1. The ST2 point charge model for water. The tetrahedral angel $\Phi_{Td}=109°\ 28'$ and q=0.23e.

The ST2 water model (Fig. 1) developed by Stillinger and Rahman (ref. 1) is a four point charge model with the charges arranged tetrahedrally around the oxygen atom. The positive charges are located at the hydrogen atom positions at a distance of 1 Å from the oxygen atom, nearly the real distance in the water molecule. The negative charges are located at the other two vertices of the tetrahedron but at a distance of only 0.8 Å from the oxygen atom. The charges have been chosen to be 0.23 elementary charges leading to roughly the correct dipole moment of the water molecule. The tetrahedrally arranged point charges render possible the formation of hydrogen bonds in the right directions. The ST2 model is completed by adding a (12;6) Lennard-Jones (LJ) potential, the center of which is located at the oxygen atom.

In the simulations where the ST2 model is employed, the alkali and halide ions are modelled as LJ spheres with a point charge at the center (ref. 3). With these models for the two kinds of particles - water and ions - it is easy to formulate the effective pair potentials for the six different kinds of interactions: cation-cation, anion-anion, cation-anion, cation-water, anion-water, and water-water. All six pair potentials consist of an LJ term:

$$V_{ij}^{LJ}(r) = 4\varepsilon_{ij}\,[(\sigma_{ij}/r)^{12}-(\sigma_{ij}/r)^{6}] \tag{1}$$

where i and j refer either to ions or water molecules, and a Coulomb term, different for water-water, ion-water, and ion-ion interactions, given by:

$$V_{ww}^{C}(r,d_{11},d_{12}\ldots.) = S_{ww}(r)\cdot q^{2}\sum_{\alpha,\beta=1}^{4}(-1)^{\alpha+\beta}/d_{\alpha\beta} \tag{2a}$$

$$V_{\substack{+w\\(-w)}}^{C}(d_{+1},d_{+2}\ldots.) = -\sum_{(+)\alpha=1}^{4}(-1)^{\alpha}\,q\cdot e/d_{\substack{+\alpha\\(-\alpha)}} \tag{2b}$$

$$V_{\substack{++\\--\\(+-)}}^{C}(r) = +\,e^{2}/r\ . \tag{2c}$$

The switching function, $S_{ww}(r)$, in the Coulomb term of the water pair potential has been introduced by Rahman and Stillinger (ref. 4) in order to reduce unrealistic Coulomb forces between very close water molecules. d and r denote distances between point charges and LJ centers, respectively, q the charge in the ST2 model. The sign of the Coulomb term is correct if α and β are chosen to be odd for positive and even for negative charges.

The LJ parameters for the cations are taken from the isoelectronic noble gases (ref. 5). Comparing e.g. Pauling radii, it is obvious that halide ions have a larger ionic radius than the isoelectronic alkali ions. In order to describe all interactions consistently, new LJ parameters had to be determined for the halide ions on the basis of the Pauling radii. The procedure employed is given in Ref. 6. Knowing the parameters for cation-cation and anion-anion interactions, the parameters for cation-water and anion-water interactions have been determined by applying Kong's combination rules (ref. 7). The results of this procedure are given in Table 1.

TABLE 1. Lennard-Jones parameters in the pair potentials for cation-cation, anion-anion, cation-water and anion-water interactions. In the ST2 model: σ = 3.10 Å and ε = 0.317 kJ/mol.

Ion	Pauling radius [Å]	σ_{II} [Å]	ε_{II} [kJ mol^{-1}]	σ_{IW} [Å]	ε_{IW} [kJ mol^{-1}]
Li^+	0.60	2.37	0.149	2.77	0.224
Na^+	0.95	2.73	0.358	2.92	0.330
F^-	1.36	4.00	0.050	3.53	0.123
K^+	1.33	3.36	1.120	3.25	0.568
Cl^-	1.81	4.86	0.168	4.02	0.185
Rb^+	1.48	3.57	1.602	3.39	0.641
Br^-	1.95	5.04	0.270	4.16	0.215
Cs^+	1.69	3.92	2.132	3.61	0.662
I^-	2.16	5.40	0.408	4.41	0.228

In Fig. 2 the ion-water pair potentials according to Eq. (2b) and based on the LJ values given in Table 1 are shown for various alkali and halide ions. The depth and the shift in the position of the potential minima show the expected changes with increasing ion size. The curves coincide beyond about 4 Å where only Coulomb interactions remain.

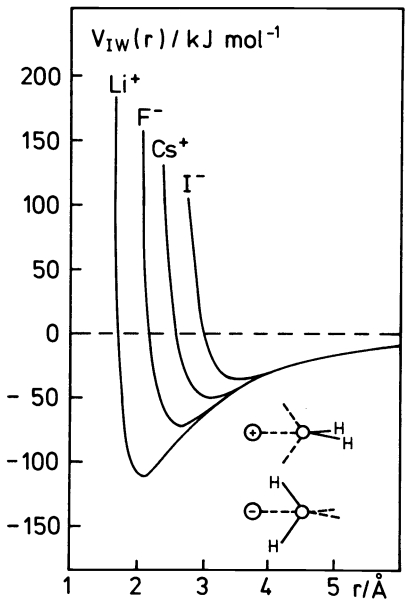

Fig. 2. Ion-water pair potentials as a function of ion-oxygen distance for selected alkali and halide ions and water molecule orientations as shown in the insertion.

TABLE 2. Potential constants used for the intramolecular part of the improved CF potential for water in units of kJ/mol (ref. 2). The notations are according to Eq. (4).

$(\rho_1^2 + \rho_2^2)$	2332.27
$\rho_1\rho_2$	- 55.7272
$(\rho_1 + \rho_2)\,\Delta\alpha$	126.242
$(\Delta\alpha)^2$	209.860
$(\rho_1^3 + \rho_2^3)$	- 4522.52
$\rho_1\rho_2(\rho_1 + \rho_2)$	- 55.7272
$(\rho_1^2 + \rho_2^2)\,\Delta\alpha$	237.696
$(\rho_1^4 + \rho_2^4)$	5383.67
$\rho_1\rho_2(\rho_1^2 + \rho_2^2)$	- 55.7272
$(\rho_1^3 + \rho_2^3)\,\Delta\alpha$	349.151

In the improved CF model for water the total potential is separated into an intermolecular and an intramolecular part. The intermolecular pair potential is an only slightly modified version of the CF model by Stillinger and Rahman (ref. 8) and is given by:

$$V_{OO}(r) = 604.6/r + 111889/r^{8.86} - 1.045\,\{\exp[-4(r-3.4)^2] + \exp[-1.5(r-4.5)^2]\} \qquad (3a)$$

$$V_{OH}(r) = -302.2/r + 26.07/r^{9.2} - 41.79/\{1+\exp[40(r-1.05)]\} \quad (3b)$$
$$-16.74/\{1-\exp[5.439(r-2.2)]\}$$

$$V_{HH}(r) = 151.1/r + 418.33/\{1+\exp[29.9(r-1.968)]\} \quad (3c)$$

The intramolecular part is based on the water potential in the formulation of Carney, Curtiss and Langhoff (ref. 9):

$$V_{intra} = \sum L_{ij}\rho_i\rho_j + \sum L_{ijk}\rho_i\rho_j\rho_k + \sum L_{ijkl}\rho_i\rho_j\rho_k\rho_l \ , \quad (4)$$

with $\rho_1 = (r_1-r_e)/r_1, \rho_2 = (r_2-r_e)/r_2$ and $\rho_3 = \alpha-\alpha_e = \Delta\alpha$, where r_1, r_2 and α are the instantaneous O-H bond lengths and H-O-H angle; the quantities r_e and α_e are the corresponding equilibrium values (r_e=0.9572 Å, α_e=104.52°). The finally adopted parameter set is given in Table 2.

With the CF model, MD simulations have been performed for a 13.9 molal LiCl (ref. 10), a 2.2 molal NaCl (ref. 11), a 1.1 molal $MgCl_2$ (ref. 12), and a 1.1 molal $CaCl_2$ (ref. 13) solution. The ion-oxygen, and ion-hydrogen pair potentials were derived from ab initio calculations and are given in Table 3. The Li^+-water, Na^+-water, and Cl^--water pair potentials derived in this way are very similar to the ones calculated from Eq. 2b and Table 1.

TABLE 3. Ion-oxygen and ion-hydrogen pair potentials employed in the simulations with the CF model for water. Energies are given in kJ/mol and distances in Å:

$$V_{LiO}(r) = -916.5/r - 488.3/r^2 + 90.27 \cdot 10^3 \exp(-3.93r)$$
$$V_{LiH}(r) = 458.2/r + 236.9/r^2 + 11.50 \cdot 10^3 \exp(-5.87r)$$
$$V_{NaO}(r) = -916.5/r - 153.6/r^2 + 48.93 \cdot 10^4 \exp(-4.53r)$$
$$V_{NaH}(r) = 458.2/r + 31.31/r^2 + 41.68 \cdot 10^4 \exp(-7.07r)$$
$$V_{MgO}(r) = -1832/r - 890.7/r^2 + 26.95 \cdot 10^4 \exp(-4.08r)$$
$$V_{MgH}(r) = 916.5/r + 82.02/r^2 + 73.83 \exp(-0.349r)$$
$$V_{CaO}(r) = -1832/r - 1572/r^2 + 25.97 \cdot 10^4 \exp(-3.49r)$$
$$V_{CaH}(r) = 916.5/r + 626/r^2 + 12.02 \cdot 10^4 \exp(-6.79r)$$
$$V_{ClO}(r) = 916.5/r - 111.3/r^2 + 37.96 \cdot 10^4 \exp(-3.21r)$$
$$V_{ClH}(r) = -458.2/r + 18.90 \cdot 10^{25} \exp(-34r)$$

DETAILS OF THE SIMULATIONS

In this paper results of MD simulations of aqueous alkali halide and alkaline earth chloride solutions are reported. In all cases the basic periodic cube contained 200 water molecules, 8 anions and 8 or 4 cations equivalent to 2.2 or 1.1 molal solutions. The sidelength of the cube is determined from the experimental density and amounts to about 20 Å for all solutions. The classical equations of motion are integrated in time steps of about $2\cdot10^{-16}$s. The simulations extended over about 10 ps.

In the simulation of the alkali halide solutions, the Ewald summation (ref. 14) is employed for the ion-ion interactions, while the ion-water and water-water interactions are cut-off at a distance of about 10 Å, half of the sidelength of the basic cube. This simple cut-off procedure leads to jumps in the potential energy and the forces each time a particle crosses the cut-off sphere and results in trends in the total energy of the system. To overcome this problem, the so-called "shifted force potential" as proposed by Streett et al. (ref. 15) has been employed (ref. 16). In the simulations with the CF model of water, the Ewald method is employed for all Coulomb interactions while for the other parts of the potential again the shifted force potential method is used. With this procedure, the energy change $\Delta E/E$ during the total simulation was smaller than $5\cdot10^{-5}$ in all cases and the average temperature remained constant without rescaling, which is very important for the reliability of the dynamical properties calculated from velocity autocorrelation functions. This modification of the pair potentials seems to be acceptable in view of all the other uncertainties in the choice of the potentials.

RESULTS AND DISCUSSION

Radial distribution functions

The first properties derived from an MD simulation as far as the structure of an aqueous electrolyte solution is concerned are the various radial distribution functions (RDF), $g_{xy}(r)$. In Fig. 3 the ion-oxygen and ion-hydrogen RDFs are shown for various alkali and halide ions. In addition, the corresponding running integration numbers, $n_{xy}(r)$, are drawn. They are defined as:

$$n_{xy}(r) = 4\pi\rho_o \int_0^r g_{xy}(r')\, r'^2 dr' \,, \qquad (5)$$

where ρ_o is the number density of the water molecules.

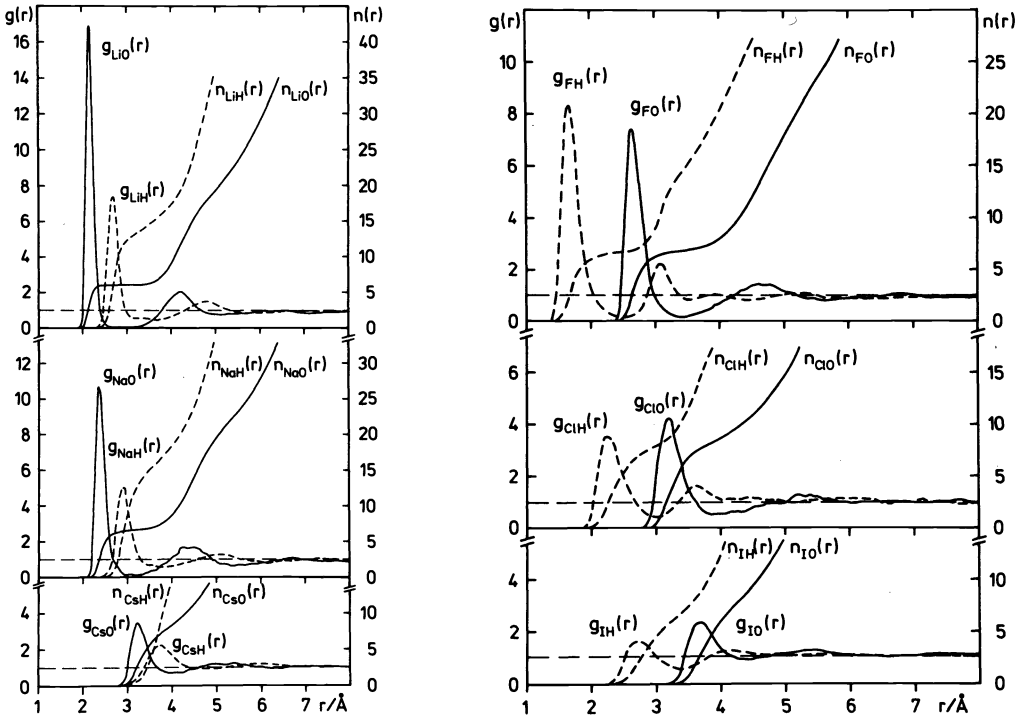

Fig. 3. Ion-oxygen (full) and ion-hydrogen (dashed) radial distribution functions and running integration numbers from MD simulations of 2.2 molal LiI (ref. 17), $NaClO_4$ (ref. 18), NH_4Cl (ref. 16) and CsF (ref. 19) solutions.

Fig. 3 shows that with increasing ion size the first hydration shell becomes less pronounced, as expected. The height of the first peak in the ion-oxygen RDF decreases and the first minimum gets filled up. Accordingly, the plateau in n(r) disappears and the end of the first hydration shell becomes less well defined. The existence of a second hydration shell around Li^+ with about twelve water molecules is well established and has been confirmed by X-ray diffraction studies as discussed below. Even in the case of Na^+ and F^- the formation of a second shell is indicated in Fig. 3. It should be mentioned that the positions of the first maxima in the ion-oxygen RDFs almost coincide with the minima of the ion-water pair potentials for the energetically most favorable orientations.

In Table 4 three characteristic values of RDFs - positions of the first maxima in the ion-oxygen and ion-hydrogen RDF and the hydration number - from three different computer simulations of various alkali and halide ions are compared. In the MD simulations of the 2.2 molal solutions, the ST2 model is employed and the ions are described as LJ-spheres with an elementary charge at the center (Eqs. 2a-c and Table 1). In the Monte Carlo calculations by Mezei and Beveridge (ref. 20) as well as in the MD simulations of Impey, Madden and McDonald (ref. 21), the MCY model for water (ref. 22) is used and the ion-water interactions are derived from ab initio calculations by Kistenmacher, Popkie and Clementi (ref. 23). It is very satisfactory to note that

TABLE 4. Comparison of characteristic values of the radial distribution functions for various alkali and halide ions. $r_{IO}^{(M)}$ and $r_{IH}^{(M)}$ denote the positions of the first maxima in the ion-oxygen and ion-hydrogen RDF, respectively. The hydration number is defined - according to Eq. (5) - as n at the position of the first minimum, $r_{IO}^{(m)}$.

Ion	$r_{IO}^{(M)}$			$n(r_{IO}^{(m)})$			$r_{IH}^{(M)}$		
	MD[a]	MC[b]	MD[c]	MD[a]	MC[b]	MD[c]	MD[a]	MC[b]	MD[c]
Li^+	2.13	2.10	1.98	6.1	6.0	5.3	2.68	2.70	2.57
Na^+	2.36	2.35	2.29	6.5	6.0	6.0	2.90	2.89	2.95
K^+	-	2.71	2.76	-	6.3	7.5	-	3.19	3.35
Cs^+	3.22	-	-	7.9	-	-	3.72	-	-
F^-	2.64	2.60	2.67	6.8	4.1	5.8	1.65	1.68	1.73
Cl^-	3.22	3.25	3.29	8.2	8.4	7.2	2.24	2.25	2.35
I^-	3.68	-	-	8.7	-	-	3.40	-	-

[a] 2.2 molal solutions of LiI (ref. 17), $NaClO_4$ (ref. 18), CsF (ref. 19) and NH_4Cl (ref. 16).
[b] One ion surrounded by 215 water molecules (ref. 20).
[c] One ion surrounded by 64 or 125 water molecules (ref. 21).

good agreement exists between the MD simulations of the 2.2 molal solutions and the MC calculations for all three properties and all ions shown in the table - except for the hydration number of F^- where the value from the MC simulation seems to be too small - although a basically different approach has been applied in the calculations of the pair potentials employed. It is surprising that the results of the MD simulations of Impey, Madden and McDonald show some significant differences although they used the same pair potentials as employed in the MC calculations. These differences might have to be attributed to the different number of water molecules used in the simulations. However, the authors report that they got the same results for the simulations with 64 and 125 water molecules.

After general agreement has been found between various simulations as far as alkali and halide ions are concerned, the question arises how the results of the simulations compare with diffraction studies. A 1.1 molal $CaCl_2$ and a 13.9 molal LiCl solution have been chosen as examples for comparison with neutron and X-ray diffraction studies, respectively.

In Fig. 4 the Ca^{2+}-water RDF from the simulation (ref. 13) is compared with the one from neutron diffraction experiments with isotopic substitution which render possible the direct determination of separate cation-water and anion-water radial distribution functions (ref. 24). There is good agreement in respect to the position of the maxima and minima. (The additional waves in the experimental RDF in the range between 3.5 and 5 Å are artificial). But the simulation results in a more pronounced hydration shell around Ca^{2+} than could be concluded from the measurements, although both agree in a hydration number of about nine. In order to check if this discrepancy persists in the structure function, the difference functions for the two calcium isotopes are shown in Fig. 5. The figure gives the results for a 4.5 molal $CaCl_2$ solution as for the 1.1 molal one the experimental $\Delta_{Ca}(k)$ is not available from the literature. The dots indicate the original data while the dashed line is the smoothed curve through them on which the experimental RDF shown in Fig. 4 is based (ref. 25). The full line shows the result of the simulation rescaled for a concentration of 4.5 molal (ref. 13). It can be concluded from the comparison that the experimental data do not necessarily exclude the result from the simulation. It has been demonstrated before that for the Cl^--water RDF the agreement between the simulation and neutron diffraction measurements with isotopic substitution is even better than in the case of Ca^{2+} (ref. 26).

Separate ion-water RDFs can be derived from X-ray measurements only by fitting a model to the experimental structure function. For the comparison with MD simulations, such procedures have been performed for various solutions

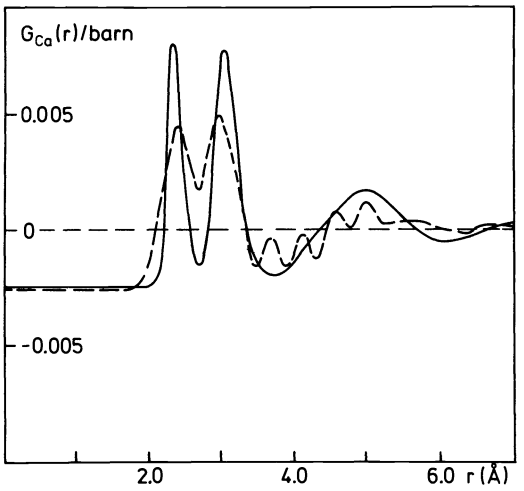

Fig. 4. Ca^{2+}-water radial distribution function for a 1.1 molal $CaCl_2$ solution from the simulation (full) and from neutron diffraction measurements (dashed).

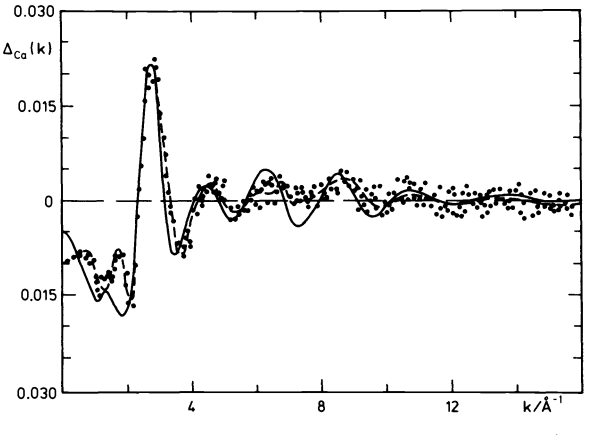

Fig. 5. Structure function difference for a 4.5 molal $CaCl_2$ solution from neutron diffraction measurements with calcium isotope substitution. Experimental data (dots, dashed curve) and rescaled results from a simulation of a 1.1 molal $CaCl_2$ solution (full).

(refs. 6,27-29) and will not be discussed here. In Fig. 6 the structure function for a 13.9 molal LiI solution from the MD simulation (ref. 10) is compared with that from X-ray diffraction. Satisfactory agreement is obtained between them, although some discrepancies are found at a higher k region (> 12 Å^{-1}) where the X-ray diffraction data might contain relatively large uncertainties due to low scattered intensities. The resulting X-ray weighted total RDFs are compared in Fig. 7. The agreement between the calculated and experimentally obtained $G(r)_x$ is again satisfactory, as expected from Fig. 6, although a difference is found at a peak around 2 Å, where mainly interactions between Li^+ and water molecules contribute.

The agreement between diffraction studies and MD simulations as demonstrated in these two examples suggests that the intermolecular configurations obtained from the simulations reproduce sufficiently the real systems. This result is especially satisfying as the parameters for the ion-water interactions employed in the simulations have not been adjusted to experimental data. They are taken either from the LJ parameters of the noble gases or based on ab initio calculations.

The effect of pressure at constant temperature on the hydration shells of

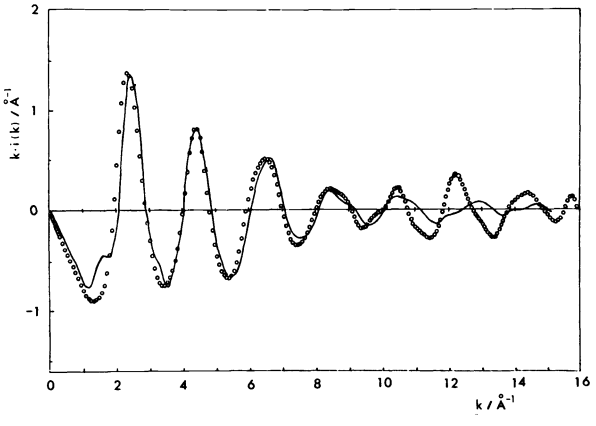

Fig. 6. X-ray structure functions for a 13.9 molal LiCl solution from experiment (dots) and MD simulation (full) (ref. 10).

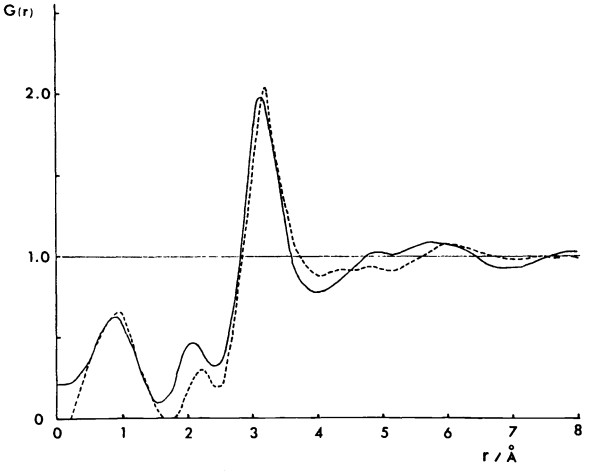

Fig. 7. X-ray weighted radial distribution functions for a 13.9 molal LiCl solution from experiment (dashed) and MD simulation (full) (ref. 10).

ions has been investigated in the case of a 2.2 molal NaCl solution. An increase in pressure of about 10 kbar resulted in only small changes in the ion-oxygen and ion-hydrogen RDFs (ref. 30). Simulations of 0.55 molal LiI solutions at constant density and temperatures of 300 K and 500 K, where the higher temperature corresponds to a pressure of about 3 kbar, showed a significant decrease in the height of the first peak in the Li^+-O RDF and an almost complete disappearance of the second hydration shell, while only small changes resulted for the Cl^--O RDF (ref. 31).

In Fig. 8 the ion-ion RDFs from the simulation of a 2.2 molal CsF solution (ref. 19) are depicted together with the running integration numbers. The strong noise results from the small number of ions in the basic cube. The $g_{CsCs}(r)$ and $g_{FF}(r)$ seem to have no significant structure outside of statistical noise. They indicate that the nearest distance of approach of two like ions is the one where the two ions are separated by just one water molecule. The Cs^+-F^- RDF is of special interest as the CsF solution was the only alkali halide solution investigated by us so far, where the simulation indicated a possible formation of contact ion pairs. But even this simulation, which extended over 6.5 ps, does not give a definite answer. If the small bump in $g_{CsF}(r)$ at about 3.5 Å can be taken seriously, it would mean that about one out of ten ions is paired. There seems to be a peak in $g_{CsF}(r)$ between 5-6 Å outside of statistical noise indicating the existence of Cs^+ and F^- which are separated by just one water molecule. Similar configurations of unlike ions have been found in the simulation of a LiI solution, too (ref. 17).

Orientation of the water molecules

The distributions of cos Θ for the water molecules in the first hydration shells of various alkali and halide ions from MD simulations of 2.2 molal LiI (ref. 17), $NaClO_4$ (ref. 18), NH_4Cl (ref. 16) and CsF (ref. 19) solutions are shown in Fig. 9, where Θ is defined in the insertion. It is obvious from Fig. 9 that a strong preference exists for a lone pair orientation of the water molecules towards the cations, while in the case of the anions preferentially linear hydrogen bonds are formed. As expected, the width of the distributions strongly increases with increasing ion size leading for the large ions (Cs^+, I^-) even to energetically unfavorable orientations.

The results presented in Fig. 9 are derived from simulations where the ST2 water model was employed. Simulations of a 2.2 molal NaCl (ref. 11) and a

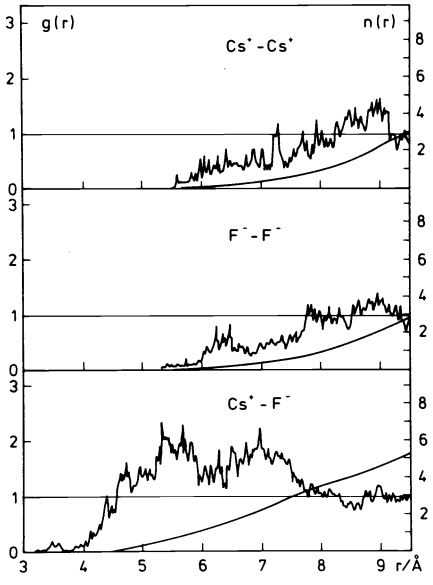

Fig. 8. Ion-ion radial distribution functions and running integration numbers for a 2.2 molal CsF solution (ref. 19).

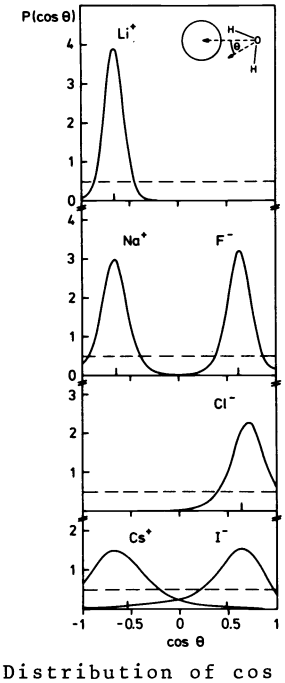

Fig. 9. Distribution of cos Θ for the water molecules in the first hydration shells of various alkali and halide ions. Θ is defined in the insertion. The dashed lines indicate uniform distributions.

1.1 molal $MgCl_2$ (ref. 12) solution with the CF model for water have led to trigonal orientations for Na^+ and Mg^{++} while for Cl^- the preference for the linear hydrogen bond formation remained (Fig. 10). Similarly, trigonal orientations have been found for Li^+, Na^+ and K^+ in the MC calculation of Mezei and Beveridge (ref. 20) with the MCY potential for water. Thus, the orientation of the water molecules in the first hydration shells of the ions is one of the rare cases where the results of the simulations depend upon the water model employed. The reason for this discrepancy might be that in the ST2 model the directionality of the lone pair orbitals is exaggerated by the negative point charges.

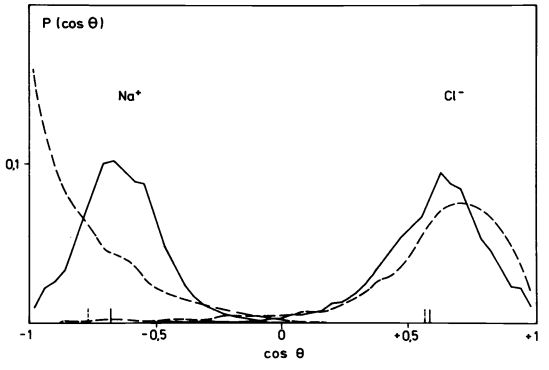

Fig. 10. Distribution of cos Θ for the water molecules in the first hydration shells of Na^+ and Cl^- from simulations of 2.2 molal NaCl solutions with the ST2 model (full) and the CF model (dashed) for water (ref. 11).

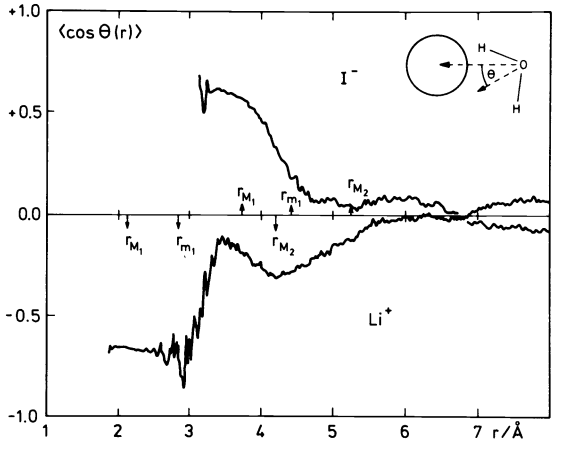

Fig. 11. Average value of cos Θ as a function of distance from the iodide and the lithium ion from an MD simulation of a 2.2 molal LiI solution. r_{M1}, r_{M2} and r_{m1} indicate the position of the first and second maximum and the first minimum in the ion-oxygen RDF, respectively (ref. 17).

The orientation of the water molecules in the hydration shells of the ions could be calculated from the distances of the first maxima in the ion-oxygen and ion-hydrogen RDFs. Only in this way information on the orientation of the water molecules can be deduced from diffraction studies. The difficulties connected with this approach have been discussed in detail in Ref. 26. For the MD simulations these difficulties do not exist as the orientations can be calculated immediately from the data produced.

The preferential orientation of the water molecules decreases rapidly beyond the first hydration shells. This can be seen from Fig. 11 where the average value of cos Θ is shown as a function of distance from the ion for Li^+ and I^- as example. Beyond about 4.5 Å the preferential orientation disappears except for the small ions which form a second hydration shell.

Hydration shell symmetries

From the knowledge of the position of all particles as a function of time, provided by the MD simulation, the ensemble and time-averaged geometrical arrangement of the water molecules in the first hydration shells of the ions can be deduced. In order to achieve this aim, a coordinate system has been introduced where the ion defines the origin, one oxygen atom of the hydration shell water molecules the z-axis and a second one the xz-plane. The number of water molecules considered to belong to the first hydration shell is $n(r_{10}^{(m)})$ where n(r) is defined in Eq. (5) and $r_{10}^{(m)}$ indicates the position of the first minimum in the corresponding ion-oxygen RDF. The registration of the water positions in the ion-centered coordinate systems at several hundred different times spread over the whole simulation run provides the average distribution of the water molecules in the hydration shells.

In Fig. 12. the projections of the oxygen atom positions onto the xy-plane for various ions are shown in form of threedimensional drawings. The figure shows unambiguously that the six water molecules in the first hydration shell of Mg^{++} are arranged octahedrally with practically no distortion and only a narrow distribution around the octahedral positions. With decreasing charge and/or increasing size of the cations, the distributions around the octahedral positions broaden resulting in a uniform distribution of the eight water molecules around Cs^+. Except for F^-, where a small preference for the occupations of the octahedral sites is indicated, for all other anions investigated a uniform distribution results.

It was concluded from the simulation of a 2.2 molal NaCl solution at 10 kbar (ref. 30) that the effect of pressure at constant temperature on the ion-oxygen and ion-hydrogen RDFs is rather small. The same simulation showed that the hydrogen bond structure of water changes significantly with increasing pressure. In Fig. 13 the distribution of the oxygen atom positions of the eight nearest-neighbor water molecules around a central one onto the xy-plane

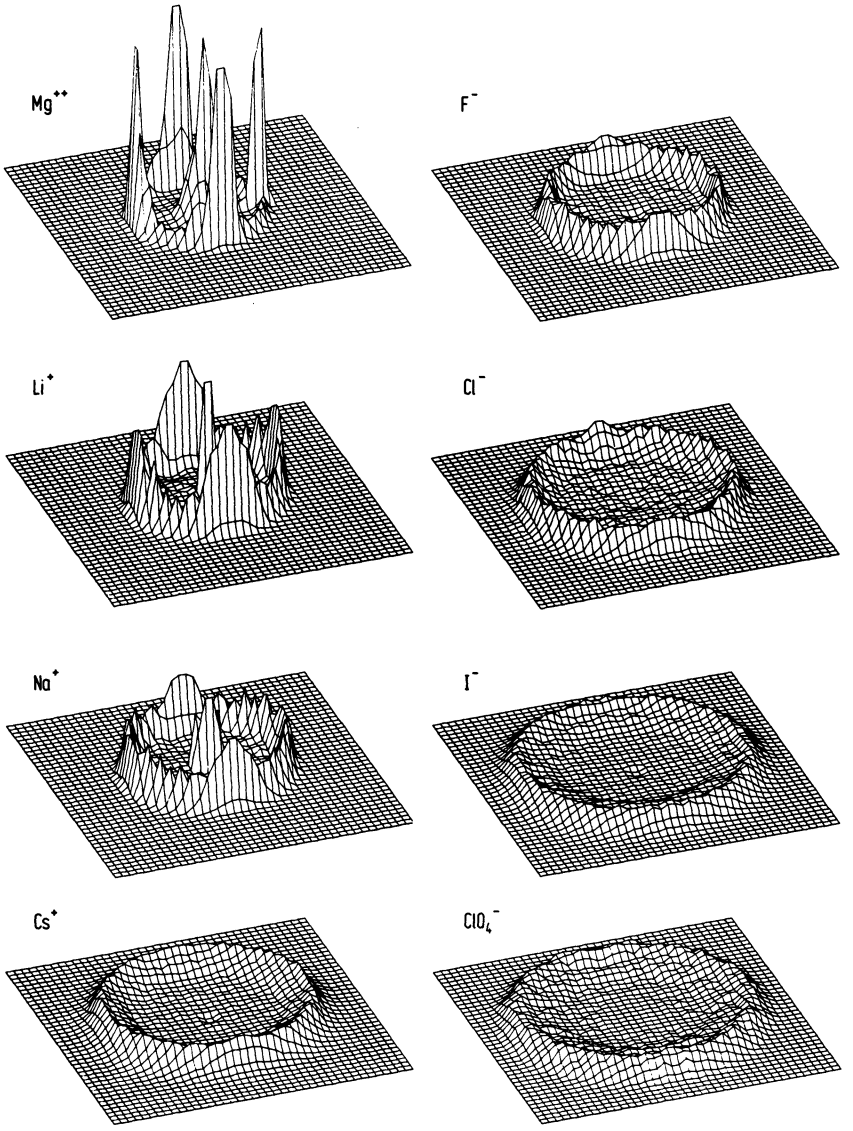

Fig. 12. Three-dimensional drawings of the projections of the oxygen atom positions of the six and eight nearest-neighbor water molecules around a Mg^{++}, Li^+, Na^+, F^- and Cl^- and a Cs^+, I^- and ClO_4^-, respectively, onto the xy-plane of a coordinate system as defined in the text. The drawings are calculated from MD simulations of a 1.1 molal $MgCl_2$ (ref. 12) as well as 2.2 molal CsF (ref. 19), LiI (ref. 17), and $NaClO_4$ (ref. 18) solutions.

of a coordinate system as defined in the insertion are depicted for normal and high pressure, again in form of threedimensional drawings. (Eight resulted as the number of nearest neighbors from the simulation of high density water (ref. 32)). It is obvious from Fig. 13 that, in the normal pressure case, the four nearest-neighbor water molecules are arranged tetrahedrally with a narrower distribution in the hydrogen atom directions while the second four are uniformly distributed at a slightly larger distance. In the high pressure case all eight water molecules belong to one shell and necessarily the preference for a tetrahedral arrangement is strongly decreased.

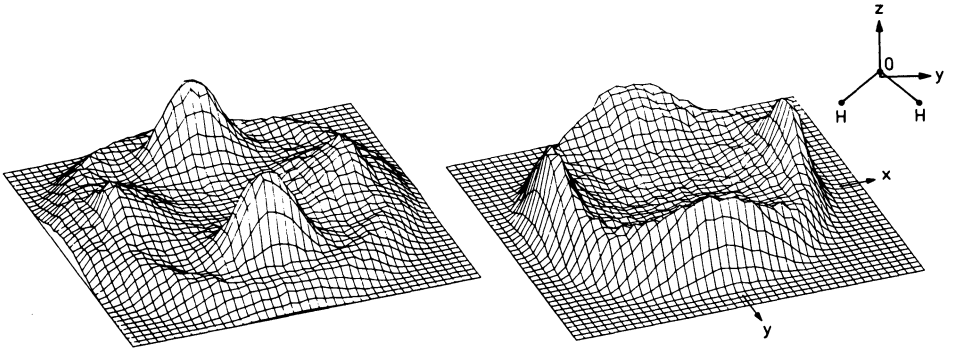

Fig. 13. Threedimensional drawings of the projections of the oxygen atom positions of the eight nearest-neighbor water molecules around a central one onto the xy-plane of a coordinate system as defined in the insertion, calculated from MD simulations of a 2.2 molal NaCl solution at low (left) and high (right) pressure (ref. 30).

Water molecule geometry

The use of the CF model permits the investigation of the influence of the ions on the geometry of the water molecules. The separate calculation of the average value of the ∢ HOH for the three water subsystems in the $MgCl_2$ solution - bulk water, hydration water of Mg^{++} and Cl^- - leads to a 5° smaller angle in the hydration water of Mg^{++} compared with bulk water. This decrease results from the repulsive forces exerted from the ion on the hydrogens and the attractive ones on the oxygen. The differences in the HOH angle lead to differences in the dipole moments which have been calculated to be 2.00, 2.01 and 2.11 D for bulk water, hydration water of Cl^- and Mg^{++}, respectively (ref. 12).

Besides the changes of the ∢ HOH, the ions also influence the average O-H distance resulting in shifts of the O-H stretching frequencies in the order of 20000 $cm^{-1}/Å$ (ref. 34). From the simulation of a 1.1 molal $CaCl_2$ solution (ref. 13), the normalized velocity autocorrelation functions of the hydrogen atoms have been calculated separately for bulk water, hydration water of Ca^{++} and Cl^-. The spectral densities of the O-H stretching vibration resulting from their Fourier transformations are shown in Fig. 14 (ref. 33). The shift in the position of the maxima between pure water and the total water of the solution (Fig. 14a) is within the limits of error which is estimated to be ± 10 cm^{-1}. This result is in agreement with Raman spectroscopic investigations (ref. 35). The spectral densities for the three water subsystems in the $CaCl_2$ solution are given in Fig. 14b. They are normalized and therefore, do not

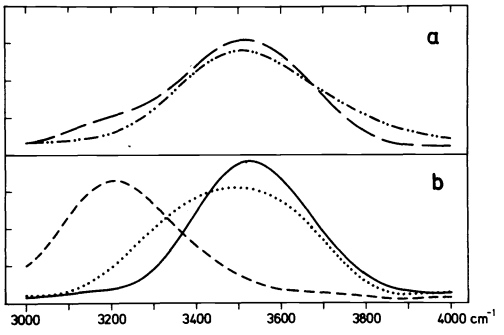

Fig. 14. Normalized spectral densities in the range of the O-H stretching frequencies of water in arbitrary units from MD simulations of pure water and of a 1.1 molal $CaCl_2$ solution. Pure water (-..-..-), total water of the solution (— —), bulk water (———), hydration water of Cl^- (·····) and of Ca^{++} (- - -) (ref. 33).

reflect the number of water molecules in the subsystems. (In the 1.1 molal solution their ratio is roughly 1:2:3 for hydration water of Ca^{++}, of Cl^- and bulk water). Their maxima are shifted by -17 cm^{-1} for bulk water, -15 cm^{-1} for hydration water of Cl^- and -302 cm^{-1} for hydration water of Ca^{++} relative to pure water. The large shift of the O-H stretching frequency of about -300 cm^{-1} for the water molecules in the first hydration shell of Ca^{++} is rather unexpected. This single ion effect cannot be derived unambiguously from infrared or Raman spectroscopic investigations.

Financial support by Deutsche Forschungsgemeinschaft is gratefully acknowledged.

REFERENCES

1. F.H. Stillinger and A. Rahman, J. Chem. Phys. 60, 1545-1557 (1974).
2. P. Bopp, G. Jancsó and K. Heinzinger, Chem. Phys. Letters 98, 129-133 (1983).
3. K. Heinzinger and P.C. Vogel, Z. Naturforsch. 29a, 463-475 (1976).
4. A. Rahman and F.H. Stillinger, J. Chem. Phys. 55, 3336-3359 (1971).
5. W. Hogervørst, Physica 5, 59-89 (1971).
6. G. Pálinkás, W.O. Riede and K. Heinzinger, Z. Naturforsch. 32a, 1137-1145 (1977).
7. C.L. Kong, J. Chem. Phys. 59, 2464-2467 (1973).
8. F.H. Stillinger and A. Rahman, J. Chem. Phys. 68, 666-670 (1978).
9. G.D. Carney, L.A. Curtiss and S.R. Langhoff, J. Mol. Spectr. 61, 371-381 (1976).
10. P. Bopp, I. Okada, H. Ohtaki and K. Heinzinger, Z. Naturforsch. 40a, 116-125 (1985).
11. P. Bopp, W. Dietz and K. Heinzinger, Z. Naturforsch. 34a, 1424-1435 (1979).
12. W. Dietz, W.O. Riede and K. Heinzinger, Z. Naturforsch. 37a, 1038-1048 (1982).
13. M.M. Probst, T. Radnai, K. Heinzinger, P. Bopp and B.M. Rode, J. Phys. Chem. 89, 753-759 (1985).
14. P.P. Ewald, Ann. Physik 64, 253-287 (1921).
15. W.B. Streett, D.J. Tildesly and G. Saville, ACS Symp. Ser. 86, 144-158 (1978).
16. Gy.I. Szász and K. Heinzinger, Z. Naturforsch. 34a, 840-849 (1979).
17. Gy.I. Szász, K. Heinzinger and W.O. Riede, Z. Naturforsch. 36a, 1067-1075 (1981).
18. G. Heinje, to be published.
19. Gy.I. Szász and K. Heinzinger, Z. Naturforsch. 38a, 214-224 (1983).
20. M. Mezei and D.L. Beveridge, J. Chem. Phys. 74, 6902-6910 (1981).
21. R.W. Impey, P.A. Madden and I.R. McDonald, J. Phys. Chem. 87, 5071-5083 (1983).
22. O. Matzuoka, E. Clementi and M. Yoshimine, J. Chem. Phys. 64, 1351-1361 (1976).
23. H. Kistenmacher, H. Popkie and E. Clementi, J. Chem. Phys. 59, 5842-5848 (1973).
24. N.A. Hewish, G.W. Neilson and J.E. Enderby, Nature 297, 138-139 (1982).
25. S. Cummings, J.E. Enderby and R.A. Howe, J. Phys. C: Solid St. Phys. 13, 1-8 (1980).
26. Gy.I. Szász, W. Dietz, K. Heinzinger, G. Pálinkás and T. Radnai, Chem. Phys. Letters 92, 388-392 (1982).
27. T. Radnai, G. Pálinkás, Gy.I. Szász and K. Heinzinger, Z. Naturforsch. 36a, 1076-1082 (1981).
28. G. Pálinkás, T. Radnai, Gy.I. Szász and K. Heinzinger, J. Chem. Phys. 74, 3522-3526 (1981).
29. G. Pálinkás, T. Radnai, W. Dietz, Gy.I. Szász and K. Heinzinger, Z. Naturforsch. 37a, 1049-1060 (1982).
30. G. Jancsó, K. Heinzinger and T. Radnai, Chem. Phys. Letters 110, 196-200 (1984).
31. Gy.I. Szász and K. Heinzinger, Earth Planet. Sci. Lett. 64, 163-167 (1983).
32. G. Jancsó, P. Bopp and K. Heinzinger, Chem. Phys. 85, 377-387 (1984).
33. M.M. Probst, P. Bopp, K. Heinzinger and B.M. Rode, Chem. Phys. Letters 106, 317-320 (1984).
34. S.J. LaPlaca, W.C. Hamilton, B. Kamb and A. Prakash, J. Chem. Phys. 58, 567-580 (1973).
35. H. Kanno and J. Hiraishi, J. Phys. Chem. 87, 3664-3670 (1983).